



A Novel Implementation of a Color-Based Detection and Tracking Algorithm for an Autonomous Hexacopter

Jeamron Angelo Arat¹, Alvin Chua^{2,*}, Louis Adrian Dela Rosa¹, Joel Ila³, Marc Jervin Jamilla¹, Jason Renz Reyes¹, Oswald Sapang¹, and Edwin Sybingco¹

¹Electronics and Communications Engineering Department, De La Salle University, Manila, Philippines

²Mechanical Engineering Department, De La Salle University, Manila, Philippines

³Computer Technology Department, De La Salle University, Manila, Philippines

*Corresponding author: alvin.chua@dlsu.edu.ph

Received: 8th August 2019

Accepted: 26th September 2019



Abstract: The increasing popularity of Unmanned Aerial Vehicles (UAVs), and the availability of associated supporting technologies such as sensors, development toolkits, and programming libraries have expanded the application areas of UAVs via customization of its functions and features. This technological trend has encouraged hobbyists to hack into off-the-shelf commercially available drones to serve different functions with minimal additional costs. In this paper, we present the practicality of using readily available off-the-shelf components in expanding a drone's functionality by designing and implementing a real-time object-following autonomous hexacopter equipped with an on-board camera used as a primary sensor; this vision-based approach for autonomous navigation addresses the limitations of GPS-based navigation in an indoor environment. The system uses the CIE L*a*b* color space to perform color-based detection and tracking, and employs ultrasonic sensor information to avoid obstacles. In all the trials, the hexacopter was able to follow the targets 90.24% of the time, with guaranteed latency of at most two minutes.

Keywords: Autonomous Control; UAV; Color-based Detection and Tracking; Obstacle Avoidance.

Introduction

Sustained innovations in Unmanned Aerial Vehicles (UAVs) technology continue to expand the variety of application scenarios with which they can be used. One particular application is indoor navigation, which makes use of the standard on-board camera accessory of off-the-shelf commercially available drones [1] to address limitations of the more predominantly used GPS technology. GPS-based navigation becomes inaccurate when used indoors because of its reliance on satellite access. Vision-based autonomous navigation, however, is still not a readily available feature of commercial drones, and when it does, it still lacks full proximity sensing and real-time tracking [2].

The Pixhawk flight controller is an open-source microcontroller used to conveniently implement control

algorithms in drone systems [3]. It works together with its companion computer, the Mission Planner, which serves as a ground control station for the UAV [4]. The flight parameters and dynamic control of the UAV can be programmatically configured from a host computer to the Pixhawk through the Mission Planner.

Vision-based autonomous navigation may be implemented via object detection and following, and an object may be conveniently identified through its color. The color information in images can be extracted depending on a chosen color space, and candidate object regions are segmented from the foreground via simple thresholding [5].

Many implementations of color-based image thresholding and segmentation employ the Hue-Saturation-Value (HSV) color space [6]. In this paper, however, we explore the feasibility of using the CIE L*a*b* color space, noting its similarity with the human

color perception model. The segmented image is a binary image mask showing valid particle targets to be tracked. In a study conducted by [7], a quadrotor UAV was used for a color-based detection and tracking application. Real-time object detection and tracking were performed using the HSV color space through thresholding; however, an obstacle avoidance algorithm as an aid to UAV navigation was not implemented. Reference [8] performed real-time object detection and tracking through the use of color features and motion information. Their study used a stationary camera facing a scene with a static background and detected the motion pixels using optical flow information. Noise removal was performed during real-time object detection through median filtering.

The NI MyRIO is a device that has been popularly used in several project implementations; it can also be conveniently connected to a camera using a Wi-Fi network. It has various data manipulation tools available in its programming environment [9], which allow the development of a two-way communication link between two different platforms such as the Pixhawk and myRIO. Using data manipulation tools, telemetry data from the Pixhawk can be sent and loaded in the LabVIEW¹ environment to be decoded. This particular strategy was used in a study by [10] that used both Pixhawk and NI myRIO in a UAV application. In their study, a fixed-wing plane, rather than a multi-rotor UAV, was used in a search-and-rescue application scenario. A custom FPGA personality in NI myRIO was developed to implement a signaling protocol to commandeer the Pixhawk controller using NI myRIO. This communication protocol for establishing a connection between NI myRIO and the Pixhawk controller was adopted in this study, while a modified version of the FPGA personality was used to suit our application. The main difference with their study is that they only used NI myRIO for basic movement commands, i.e. autonomous take-off and landing, and they did not use image processing for autonomous navigation.

In this paper, we describe the development of a UAV system capable of autonomous navigation, that tracks and follows a target using a combination of visual information and ultrasonic proximity sensed data for obstacle avoidance. Real-time autonomous navigation is achieved by utilizing a technique that allows the Pixhawk and NI myRIO to communicate during the actual navigation.

Obstacle Avoidance

Echo-location was employed using ultrasonic sensors for obstacle detection and avoidance. Figure 1 shows the rear view of the UAV prototype, indicating where the ultrasonic sensors are placed: one facing the back, and two facing the sides of the hexacopter. Adding a front-

facing sensor is unnecessary because it might consider the target object as an obstacle rather than the object to be tracked.

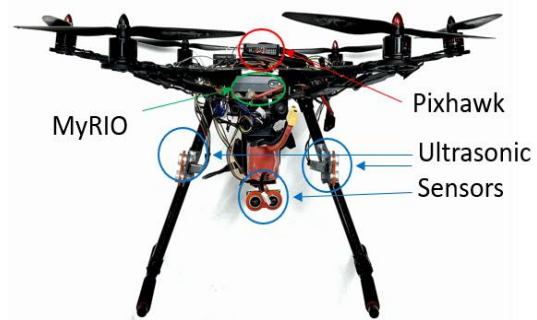


Figure 1. Hexacopter Frame (Rear View) indicating locations of the MyRIO embedded device, the Pixhawk flight controller, and ultrasonic sensors.

The ultrasonic sensors are positioned away from the frame to avoid picking up noise caused by the vibration of the motors. They are also placed in between the frame's arms and are oriented in such a way as to avoid wind interference. The two side-facing ultrasonic sensors were mounted on the legs of the frame of the hexacopter, while the third ultrasonic sensor was attached on the battery.

The flowchart of the obstacle avoidance algorithm is shown in Figure 2. Obstacle avoidance considers two cases based on a threshold distance, which is set at 1.7 meters. The first case corresponds to a reading greater than the threshold distance, wherein the hexacopter will continue to hover and follow the selected target through the color-tracking algorithm. The second case corresponds to a reading equal or below the threshold distance, which indicates that an obstacle is near.

The threshold distance was empirically determined to ensure that the hexacopter has sufficient room for movement for cases when the ultrasonic sensor reading is inaccurate, such as when the distance reading suddenly drops. Distance readings below 0.4 meters are filtered out since these distances represent the length of the actual frame of the hexacopter; therefore, a distance reading within this range is impossible to happen while the hexacopter is on flight.

When the condition for the second case has been met, the hexacopter will begin to maneuver away from the obstacle. The obstacle avoidance procedures corresponding to the two directions of movement, i.e. longitudinal and lateral, are separated and work in parallel. As a consequence, if the ultrasonic sensors have detected obstacles in both directions, the hexacopter will move away from the obstacle in these directions, which will result in a diagonal movement.

Along the longitudinal direction, two ultrasonic

¹ <http://www.ni.com/en-ph/shop/labview.html>

sensors were considered, i.e. left and right. The resultant distance of these two sensors was calculated using the formula:

$$D_x = U_{Left} - U_{Right} \tag{1}$$

Where D_x is the resultant distance, U_{Left} is the distance reading of the left ultrasonic sensor, and U_{Right} is the distance reading of the right ultrasonic sensor.

This resultant distance, which indicates the location of the obstacle, will be the basis of the movement of the hexacopter. If the resultant distance is positive, it implies that there is an obstacle at the right side of the hexacopter. On the other hand, if the resultant distance is negative, the location of the obstacle is on the left side of the hexacopter. Along the lateral direction, the ultrasonic sensor at the back is only considered. In this case, when the reading is below the threshold distance, the hexacopter will move away from the obstacle detected.

A Proportional-Integral-Derivative (PID) controller is used to control the movements of the hexacopter based on the ultrasonic sensor distance readings. LabVIEW has a ready-made virtual instrument (VI) for implementing PID control which can be modified for different applications. This VI is used and has different input parameters that must be set such as the process variable, the setpoint, and the controller gain. The process variable is the parameter that must be controlled in a system. This is typically obtained by using a sensor, e.g. ultrasonic sensor for a distance measurement, which provides feedback in a system. The setpoint is the desired value for the process variable. These two parameters are compared to obtain the error which will be the basis for the output of the controller. The PID controller with appropriate controller gain will make the necessary adjustments to provide the desired output for the system [11].

The distance readings for the back and the resultant distance were fed to the process variable of the PID controller function of LabVIEW for the lateral and longitudinal directions, respectively. A value of zero for the resultant distance of the left and right ultrasonic sensors, and the threshold distance value for the back ultrasonic sensor reading indicate that the hexacopter is not detecting any obstacle. Based on these sensor readings, the movement of the hexacopter is adjusted. When the process variable is farther from the setpoint, the output of the PID will be higher, hence the pitch and roll values will also be higher, moving away from the obstacle until it obtains the setpoint values.

A fail-safe mechanism was also implemented in the obstacle avoidance algorithm. This fail-safe scenario happens when an obstacle is detected at the back while the hexacopter is following the target. Since the priority of the hexacopter is to move away from that obstacle before following the target, it will then move forward

which also means that it will move towards the target. This is an undesirable scenario since the hexacopter may collide with the target. Therefore, when the hexacopter has detected an obstacle at the back and the target is two (2) meters away from the hexacopter, the hexacopter will commence landing to keep the target safe.

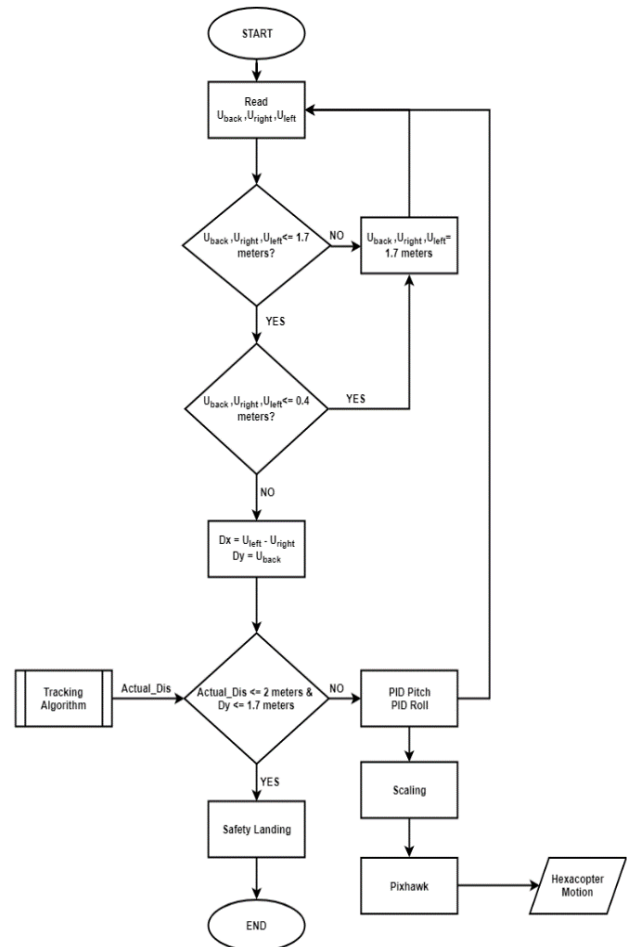


Figure 2. Flowchart of Obstacle Avoidance.

Color Detection and Tracking

For detection and tracking, a live video is sent to the ground station, which is presented in the Graphical User Interface (GUI) front panel, for target selection. A user can select by drawing a rectangular region of interest (ROI) over the video shown. Upon selection, the current frame is stored as the source frame, and a binary mask image is created from the ROI.

Detection and tracking of the target object is performed through color thresholding. In this method, each frame is processed to accept certain pixels within the specified range of color values, and reject all other pixels outside this range. For this study, thresholding is implemented using the OpenCV library, using the CIE $L^*a^*b^*$ color space. In the $L^*a^*b^*$ color space, the a^* and b^* color planes hold the color information of the image. The a^* axis represents the red/green color value (where -

a is green, and +a is red), and the b* axis represents the blue/yellow color value (where -b is blue, and +b is yellow). The L* axis represents the lightness of the colors in an image, and all values from this plane are accepted (from black 0 to white 255).

A shared library is created that does the following steps:

1. Image Conversion from RGB to CIE L*a*b*.
2. Extraction and Thresholding of the L*, a*, and b* color planes of the image based on mean and standard deviation calculations
3. Creation of a binary image resulting from the color thresholding.

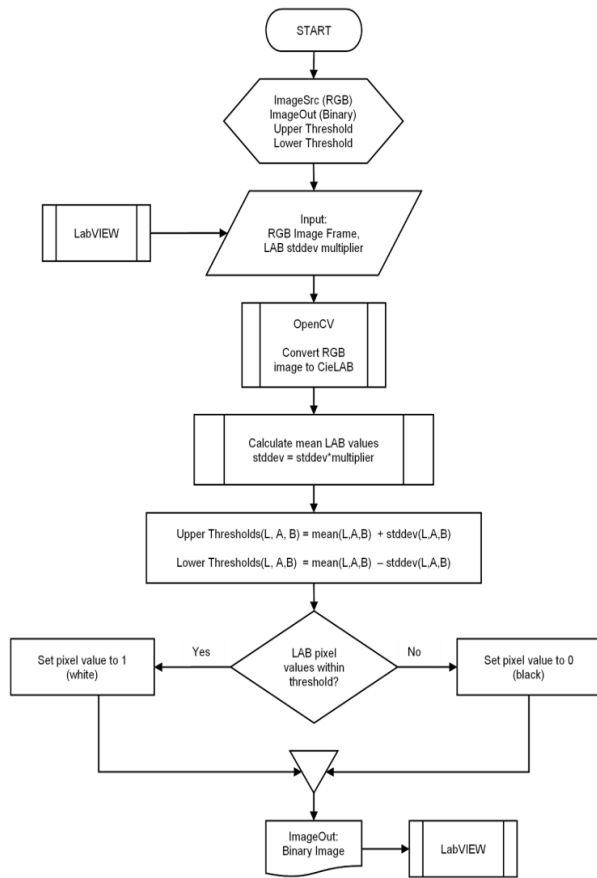


Figure 3. Flowchart of Color-Based Object Detection Stored in Shared Library.

From the LabVIEW code, the shared library is called using the Call Library Function Node and executes the code to process the image. The process flowchart of this shared library is shown in Figure 3.

After thresholding, the image is fed to image processing virtual instruments (VIs) available in LabVIEW to improve the binary image. It is first fed to the IMAQ (Image Acquisition) Particle Filter VI, which has a capability to filter or remove particles in the binary image using a measurement parameter called “%area/image”, which is the ratio of the percentage of a particle area to

the total image area (in this case, the 320 by 240 camera resolution). The VI is set to remove all particles with %area/image values between the 0 to 0.5, thus it retains the particles with large areas. The image is then fed to the IMAQ Fillhole VI which fills the holes in large particle in the binary image. Image segmentation outputs corresponding to these various phases are shown in Figure 4.

After the thresholding improvements, the image is fed to the IMAQ Particle Analysis VI to analyze the remaining particles. The VI computes and provides different particle attributes. The particle center of mass and bounding box attributes were retrieved for display and tracking.

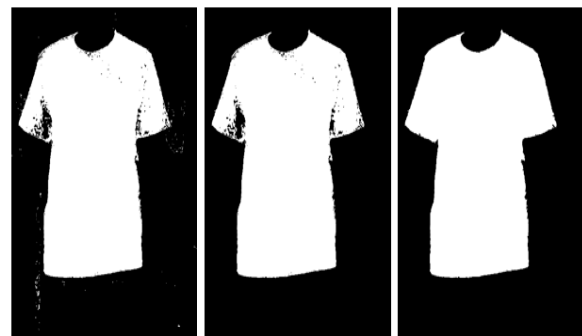


Figure 4. IMAQ Color Threshold Output (Left), IMAQ Particle Filter Output (Middle), IMAQ FillHole Output (Right). The images show increasing refinement in the segmentation output, finally resulting in a single blob corresponding to the shirt being tracked.

Refer to Figure 5 for the flowchart used for target tracking. For a single object of the desired color detected, the previous center coordinates are updated by current center coordinates. For cases wherein two or more blobs are visible after thresholding, a distance-based tracking is applied. This method calculates the Euclidean distance of all the current particles’ centers of mass from the previous frame’s target’s center of mass. The blob with the closest distance to the previous target’s center will be labeled as the target. The center of mass and the bounding box height will be used as bases for the corresponding motion of the hexacopter.

Hexacopter Motion

Obstacle avoidance is prioritized over target-following; when no obstacle is detected near and around the hexacopter, target-following proceeds. In this study, the targets are shirts worn by human subjects, effectively making the human subjects as targets for following. In this algorithm, the main objective is to maintain a specified distance from the hexacopter to the tracked target and align the center of mass of the target with the center of the image. To achieve this, both roll and pitch

are controlled using a PID controller, which gets feedback on the current center of mass of the target and the distance of the hexacopter to that target calculated using the triangle similarity for the object-to-camera distance [12]. The PID VI provided by LabVIEW is also used in controlling the hexacopter motion for following.

The focal length was first calculated by using the formula [12]:

$$F = P(D/L) \tag{2}$$

Where P is the pixel length of the shirt, D is the actual distance of the shirt to the camera, L is the actual length of the shirt and F is the focal length of the camera. The pixel length of the shirt was obtained by using the width of the bounding box which was approximately equal to the actual pixel length of the shirt. Then, the actual length of the shirt was measured at 0.68 meters. The focal length was calculated when the camera has an actual distance of three (3) meters from the shirt. In this distance, the shirt has 59-pixel length, and the focal length calculated is 260.2941. With this focal length, the approximated actual distance of the hexacopter from the shirt can be obtained through the formula:

$$D' = F(L/P) \tag{3}$$

where D' is the approximated actual distance, F is the focal length of the camera, P is the pixel length of the shirt and F is the focal length of the camera.

With this approximate distance reading, the hexacopter must be able to maintain a certain distance from the target. This maintaining distance is set at 2.5 meters. When the actual distance ishan maintaining distance, the hexacopter must move backward. When the actual distance is greater than the maintaining distance, the hexacopter must move forward.

In the PID VI, the setpoint for the roll PID controller is set at the center of the image, and the process variable is the current x-coordinate of the center of mass. For the pitch PID controller, the setpoint is set at 2.5 meters away from the hexacopter, and the process variable is the approximate distance reading calculated using the triangle similarity [12].

Once the tracked target is occluded or lost from the frame, the hexacopter will automatically commence emergency landing. For the emergency landing, the Land Mode of Pixhawk is engaged. In this mode, the throttle of the hexacopter automatically decreases but the pilot has control of the pitch, roll, and yaw to guide the hexacopter to land in a safe landing surface. The hexacopter will also engage in a “safe landing” mode whenever there is an obstacle detected at the back of the hexacopter and the target is moving towards the hexacopter within two (2) meters as explained in the Obstacle Avoidance section. The flowchart for the target following algorithm can be seen in Figure 6.

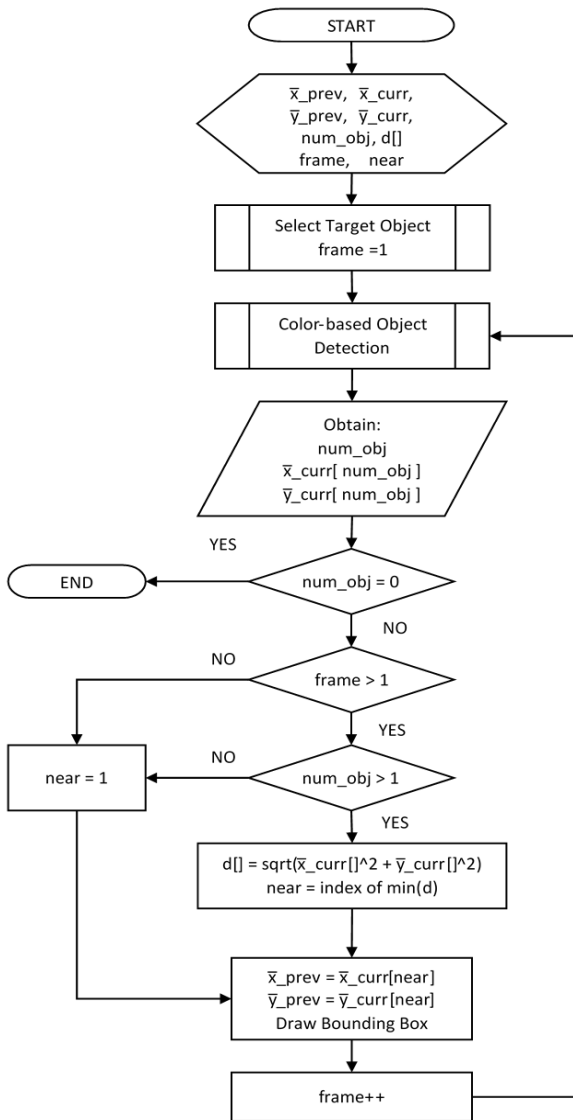


Figure 5. Flowchart of Distance-Based Tracking.

The sideward motion of the hexacopter is based on the current position of the center of mass of the target relative to the center of the image. When the center of mass is at the right, the roll of the hexacopter is adjusted by the PID to move to the right. When the center of mass is at the left, then the hexacopter roll is adjusted by the PID to move to the left.

The backward-forward movement of the hexacopter is based on the measured distance of the currently tracked target. To obtain this distance, the triangle similarity for object-to-camera was used.

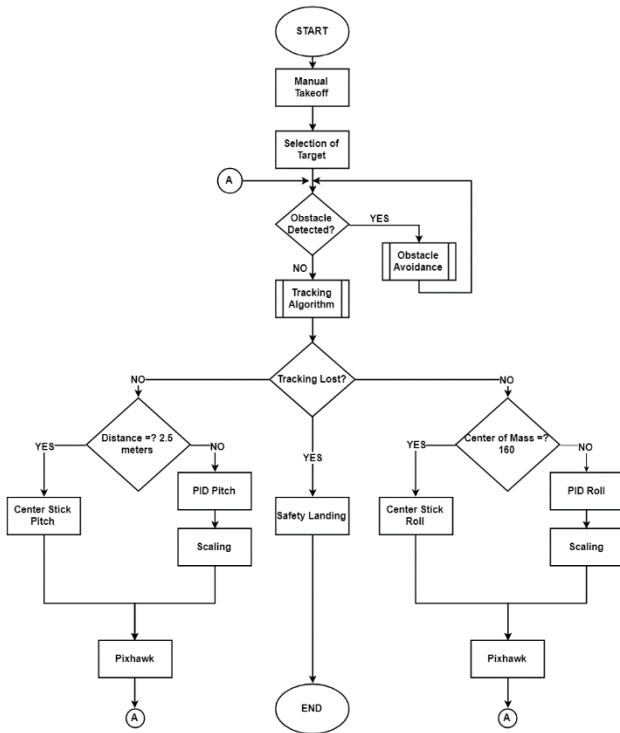


Figure 6. Flowchart of Target Following.

Experimental Setup

Figure 7 shows the general block diagram of the system. The system is comprised of the NI myRIO, camera, ultrasonic sensors, Pixhawk and a ground station (laptop) to achieve autonomous navigation of the hexacopter. Pixhawk is used as the flight controller, while the NI myRIO, connected with the camera and the ultrasonic sensors, is used for the implementation of the autonomous navigation by following the selected object through color-based detection and tracking and avoiding obstacles through the reading measurements of the ultrasonic sensors, which were all described in the previous sections. The receiver and transmitter used are the Radiolink R12DS receiver, and Radiolink AT10 transmitter, respectively. The researchers conducted flight tests and tuned the PID controller to achieve an optimal flight performance for indoor UAV navigations. During these flight sessions, a TCP connection was established between the NI myRIO and the ground station for remote data acquisition and for monitoring the on-board image processing as well as the ultrasonic sensor measurements.

The corresponding movement commands must be issued by the NI myRIO to the Pixhawk based on the output of the image processing module. Thus, communication must be established between the two devices. Since the SBUS protocol is used by the Pixhawk controller to communicate with the receiver, the myRIO device's control commands should be transmitted via this protocol. The SBUS protocol can be emulated by the FPGA

personality of the NI myRIO which allows reconfiguration of the input and output channels of the NI myRIO.

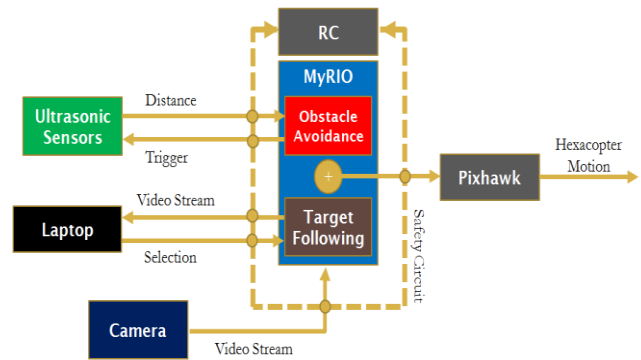


Figure 7. General Block Diagram of the System. The MyRIO embedded device receives the target object's location as selected by the user via a connection from a laptop, and processes sensor information from the ultrasonic sensors and the camera during the tracking process. It also sends commands to the Pixhawk module to direct the UAV's movement during target following.

We used the algorithms described in the Samaritan project [10], with some modifications, described below. To emulate the SBUS protocol in NI myRIO, the packet structure of the SBUS protocol must be known. The SBUS protocol uses an inverted serial logic that allows the control of motors and is capable of accommodating 16 channels with a single signal. This signal contains a start bit, start byte (0x0F) and 25 data bytes. Furthermore, this protocol uses 11 bits of data for each channel of the radio transmitter [13]. Therefore, at least two bytes of data is needed to represent a single channel. However, the Radiolink R12DS only supports 10 channels, with the first four channels used for the four main commands (roll, pitch, throttle, and yaw), and the remaining channels are used for auxiliaries (switches) [14]. The complete representation of each channel is shown in Table 1. Fourteen (14) data bytes are only used by the channel, and the remaining bytes are either used for error checking bytes or the end byte [13]. Moreover, each byte of the signal (start byte and data bytes) are appended by four more bits namely: a parity bit, two stop bits, and a start bit (in this order). With the packet structure known, each bit is produced in NI myRIO to give the corresponding movement commands.

Figure 8 illustrates the order of connection from the hexacopter's transmitter to the Pixhawk flight controller. The NI myRIO resembles a radio receiver since it can now communicate with Pixhawk using the SBUS protocol. Thus, the myRIO can now directly control the movements of the hexacopter, instead of being controlled by the radio transmitter. We did not remove the radio receiver and radio transmitter to allow manual control of the hexacopter during take-off and in emergency situations.

The pilot can override the autonomous control with this kind of setup through a switch in the radio controller. This is done to avoid accidents during testing.

Table 1. Bit Mapping of Channels in SBUS Protocol.

Channel	Data Bytes Occupied	Command
1	1st Data Byte (8) + 2nd Data Byte (3)	Roll
2	2nd Data Byte (5) + 3rd Data Byte (6)	Pitch
3	3rd Data Byte (2) + 4th Data Byte (8) + 5th Data Byte (1)	Throttle
4	5th Data Byte (7) + 6th Data Byte (4)	Yaw
5	6th Data Byte (4) + 7th Data Byte (7)	Switch C
6	7th Data Byte (1) + 8th Data Byte (8) + 9th Data Byte (2)	-
7	9th Data Byte (6) + 10th Data Byte (5)	-
8	10th Data Byte (3) + 11th Data Byte (8)	-
9	12th Data Byte (8) + 13th Data Byte (3)	Switch B
10	13th Data Byte (5) + 14th Data Byte (6)	-

Since the radio receiver is connected in NI myRIO, the NI myRIO can read the signals coming from the radio transmitter which is received by the radio receiver. When the system is in manual mode, the NI myRIO will just re-transmit the signal from the radio receiver directly to the Pixhawk. On the other hand, when the system is in autonomous mode, the NI myRIO will just read the signal coming from the radio receiver, but it will not be transmitted to the Pixhawk.

The signal that will be transmitted to the Pixhawk is based on the target following algorithm or the obstacle avoidance algorithm employed in the NI myRIO.

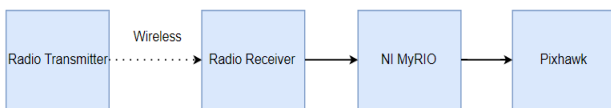


Figure 8. Order of connection from the hexacopter's radio transmitter to the Pixhawk flight controller.

Experiments and Results

The system was tested in three different ways to show its capability in tracking and following the target under different scenarios. The speed of the target during the target following is approximately 1 m/s. The hexacopter was launched manually and is maintained at

an altitude of around 1.3 meters. The tracking performance is characterized by obtaining the rate at which the hexacopter was able to maintain a distance of 2.5 meters to the target as well as its ability to maintain the center of mass of the target within the allowable range.

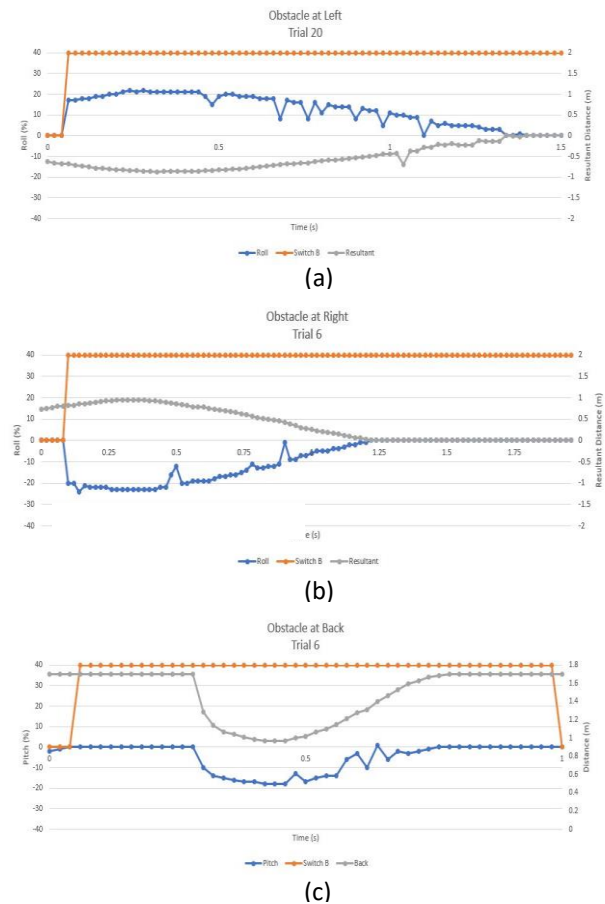


Figure 9. Ultrasonic Readings and Hexacopter Response Data when Obstacle is (a) at the Left Side; (b) at the Right Side; (c) at the Back.

The desired center of mass must be at the center of the frame, which is at an x-pixel position of 160 since the image frame resolution used is 320x240. Similarly, the distance of the hexacopter from the object must be maintained at 2.5 meters. With these desired values, a range $\pm 25\%$ of the desired value is set, with the lower and upper ranges set at pixel position 120 and position 200, respectively, for the center of mass. A lower and upper range of 1.875 meters and 3.125 meters are set, respectively, for the distance.

Furthermore, the reliability of the system is obtained by getting the percentage of the total number of successful tracking tests over the total number of tests conducted. A tracking test is considered successful when the hexacopter can follow the target at a minimum of 2 minutes.

Obstacle Avoidance Test

To test the ultrasonic sensors for obstacle avoidance, the hexacopter was initially set in manual mode and controlled by the pilot to accelerate towards an obstacle. While the hexacopter is in motion, autonomous mode with obstacle avoidance mechanism is then activated. The ultrasonic sensor logs were used to assess the hexacopter's motion response behavior in the presence of an obstacle. This test includes 30 trials of five set-ups corresponding to activations of individual and some combinations of ultrasonic sensors. The first three set-ups tested the individual ultrasonic sensors for sensing and avoiding obstacles at the left, the right, and the back of the hexacopter. The fourth set-up has a left and a rear obstacle-presence while the fifth is a combination of a right and a rear obstacle. The chosen obstacles are vertically oriented, wide, white PVC boards. Figures 9, 10 and 11 show the resulting graphs for representative trials of each set-up. Performance is evaluated by whether the hexacopter was able to avoid the obstacles and whether distances from obstacles were maintained as defined by the thresholds.

The left and the right movement of the hexacopter is controlled using the resultant distance. The resultant distance (in meters) indicates how far away is the hexacopter from the distance threshold when the hexacopter enters the danger zone.

Figures 9a and 9b show trials with obstacles detected on the left and the right, respectively. The grey line represents the resultant distance, indicating that the obstacle is located at the left when it is negative, and the obstacle is located at the right when the resultant distance is positive. The blue line represents the roll response wherein a positive value means the hexacopter must roll clockwise and move right and a negative value means roll counter-clockwise and move left. The orange line represents the switching between manual and autonomous mode represented by the values 0 and 1, respectively. Notice that the roll control responds only when the switch is in autonomous mode. The goal was to roll away from the obstacle and bring the resultant distance to zero.

Figure 9c shows a rear obstacle test, in which the ultrasonic sensor at the back of the hexacopter was evaluated. As in the case of the left and right obstacle avoidance tests, the orange line represents the switch and the blue line represents the response control (pitch) of the hexacopter. However, the grey line indicates the measured distance from the back instead of a resultant distance. The goal is to move the hexacopter at least 1.7 meters away from the obstacle. A negative pitch means a bowing movement of the hexacopter and a response to move to the front.

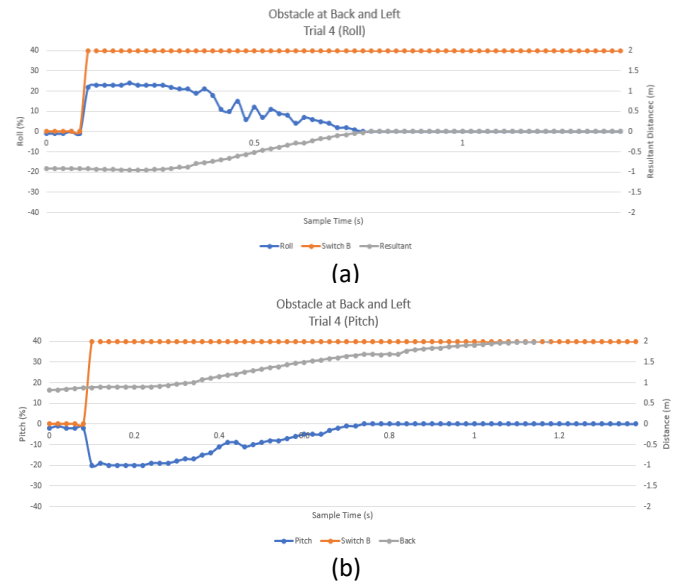


Figure 10. Ultrasonic Readings and Hexacopter Response Data when Obstacle is at the Back and at the Left Side. (a) Roll Response; (b) Pitch Response.

When the obstacles are combined (left-back or right-back obstacles), the hexacopter responded by moving away from the obstacles in both directions, i.e. diagonally away from the obstacles. This behavior is due to the obstacle avoidance mechanism responding to each ultrasonic sensor inputs simultaneously, resulting in a direction of movement as a combination of the basic left or right, and forward movements.

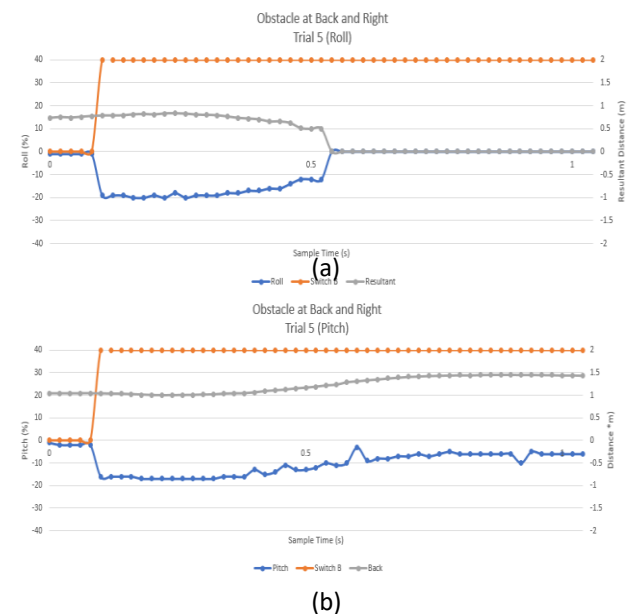


Figure 11. Ultrasonic Readings and Hexacopter Response Data when Obstacle is at the Back and at the Right Side. (a) Roll Response; (b) Pitch Response.

Figures 10 and 11 show the trials where the obstacles are placed at the back and left side, and at the

back and right side, respectively. Figures 10a and 11a show the response of the hexacopter in the longitudinal direction, while Figures 10b and 11b illustrate the hexacopter response in the lateral direction. Like the previous discussions for this test, the grey line represents the ultrasonic readings, the orange line represents the switch and the blue line represents the roll or pitch response of the hexacopter.

Major Test 1

In major test 1, the system was programmed to detect and track green objects only, and the target is moving in a predefined path without any nearby stationary obstacles. Five paths were created as shown in Figure 12, with three trials for each path. In paths 1 and 2, the object moved in straight directions only. It is either forward-backward or sideward motion, respectively. For path 3, the object is moving in an L-path, which involves both forward-backward and sideward motions, but only one at a time. For paths 4 and 5, a diagonal movement is introduced because the path is in diamond and zigzag form, respectively.

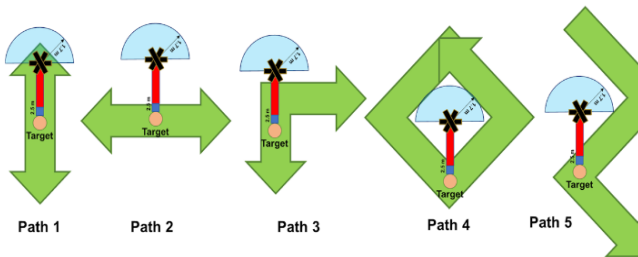


Figure 12. Five Paths for Major Test 1.

In this test, the distance calculation using the focal length of the camera was not yet implemented. Instead, this test relied on the bounding box area for estimating the actual distance of the hexacopter from the target. Also, the PID control for the pitch of the hexacopter is not fully optimized since the hexacopter has difficulty maintaining the desired distance away from the target for this major test.

The best performance of the hexacopter for maintaining the center of mass and bounding box area within the desired range occurred for Path 1 and Path 2, which only involve forward/backward movements and sideward movements, respectively. For both cases, there is only a minimal combination of movements from the roll and pitch of the hexacopter. When a change in scale is introduced along with translational motion (such as diagonal motion), the tracking of the hexacopter performed worse. This degradation in performance is evident in Path 4 which has only purely diagonal movements, wherein, the allowable distance was not maintained to the desired range for a majority of the trials conducted.

Overall, the system was able to maintain the desired range for 63.43% of the time. For the left-right (roll) movement, the hexacopter performed better and was able to maintain within the center 81.11% of the time. Figures 13 and 14 show the individual accuracies for maintaining the centers of mass and the distance at the allowable range for each path.

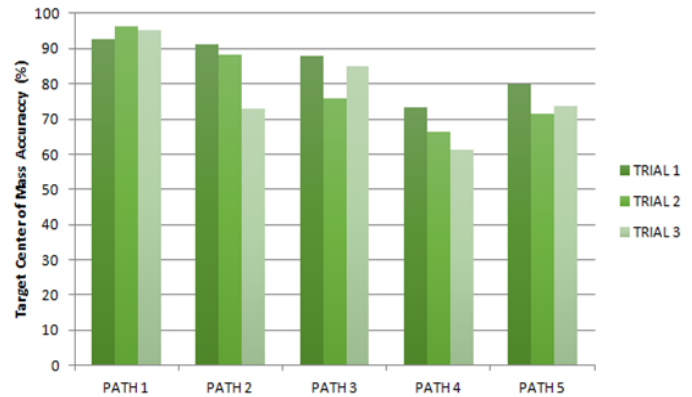


Figure 13. Target Center Accuracy for Major Test 1.

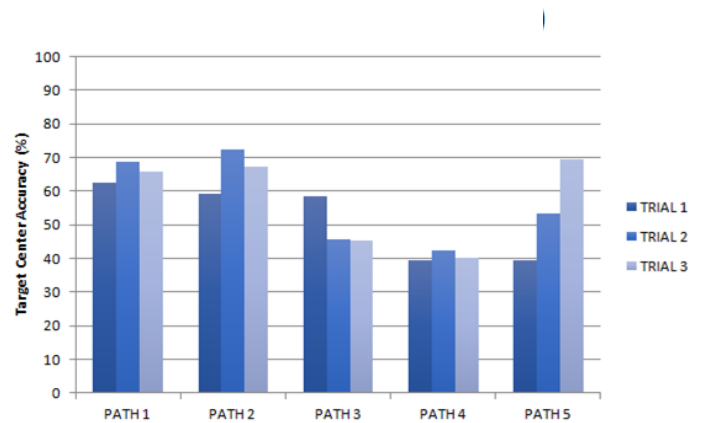


Figure 14. Target Distance Accuracy for Major Test 1.

Major Test 2

In major test 2, the system was still programmed to detect and track green objects only, but stationary obstacles were present while the target is moving. The target is moving with the same path for all the trials, but different stationary obstacles were present in three different locations (back only, left only or right only).

In major test 2, the hexacopter had successfully followed the selected target, i.e. fixed to green shirt only, with the obstacle avoidance algorithm activated. For this test, only one color (green), was used since the group primarily focused on the behavior of the movement of the hexacopter during target tracking. In this test, the PID gains are re-tuned which yielded an improved performance for maintaining its distance from the target from 63.43% to 85.42%. However, the accuracy for the

center of mass is lower compared to the previous data gathered which is only at 75.01%. The improvement in maintaining the desired distance from the selected target may come from the change in the process variable and setpoint of the PID controller. Instead of using the area of the bounding box for forward-backward motion, the distance of the target from the hexacopter is used. The distance is calculated based on triangle similarity as explained in section IV.

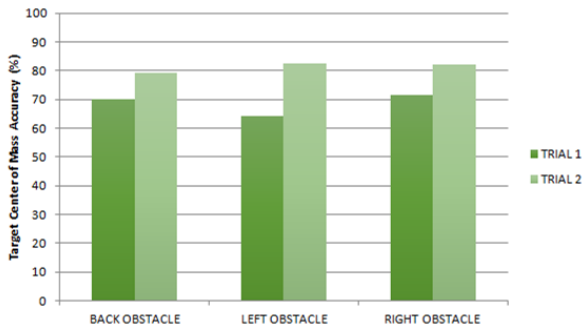


Figure 15. Target Center Accuracy for Major Test 2.

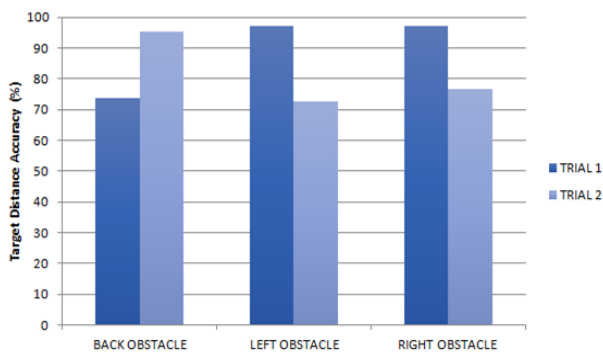


Figure 16. Target Distance Accuracy for Major Test 2.

Figures 15 and 16 show the accuracy of the system for maintaining the center of mass and the distance of the hexacopter from the target in each of the trials of each scenario.

Major Test 3

In major test 3, the color-based detection and tracking system was tested with a predefined path for the target person to navigate in a simulated indoor environment as shown in Figure 17. A total of twenty trials with four shirts of different colors were conducted for the designed path shown in Figure 18. The accuracy and efficiency performance results are shown in Table 2.

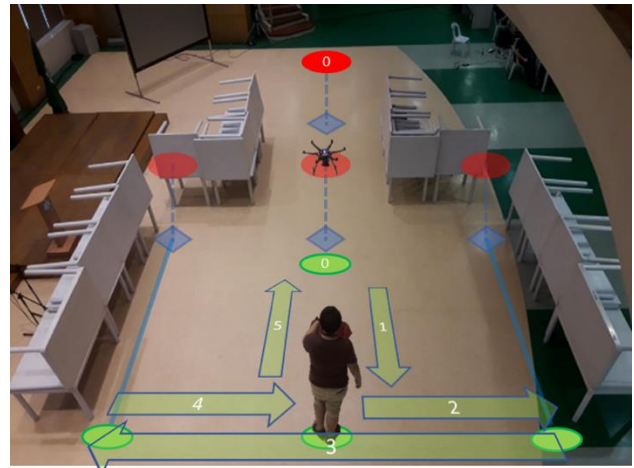


Figure 17. Testing Setup and Predefined Path



Figure 18. Shirts Used for Major Test 3.

Table 2. Major Test 3 Accuracy and Efficiency.

Target Color, Trial #	Center of Mass Accuracy (%)	Distance Accuracy (%)	Exceed 2 mins? (Y/N)
Dark Blue 1	65.07	79.48	Y
Dark Blue 2	56.81	68.08	Y
Dark Blue 3	55.93	90.03	Y
Dark Blue 4	48.75	89.23	Y
Dark Blue 5	52.87	86.55	N
Green 1	59.17	75.73	Y
Green 2	54.75	77.97	Y
Green 3	93.25	68.24	Y
Green 4	74.99	82.98	Y
Green 5	74.22	74.07	N
Light Blue 1	66.89	87.38	Y
Light Blue 2	63.31	83.66	Y
Light Blue 3	45.88	72.05	Y
Light Blue 4	65.58	78.40	Y
Light Blue 5	70.70	86.54	Y
Red 1	77.60	85.74	Y
Red 2	80.76	84.61	Y
Red 3	76.35	89.95	Y
Red 4	28.54	85.61	N
Red 5	76.61	50.66	N
Overall	64.25	79.85	16 out of 20

Presented are some of the values for the center of mass of the target as well as the measured distance of the target to the hexacopter during target following for major test 3.

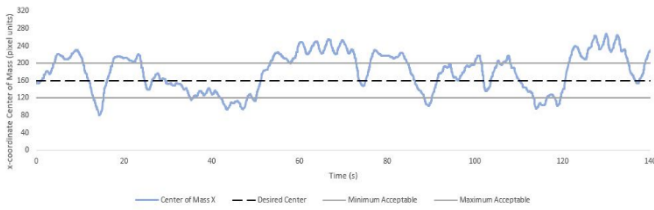


Figure 19. Center of Mass Data for Trial 3 Light Blue.

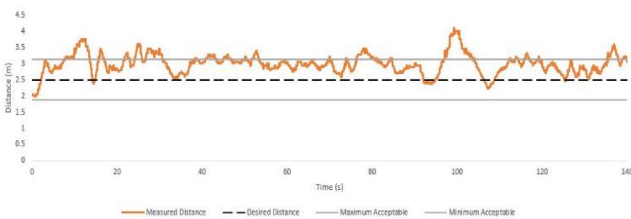


Figure 20. Measured Distance Data for Trial 3 Light Blue.

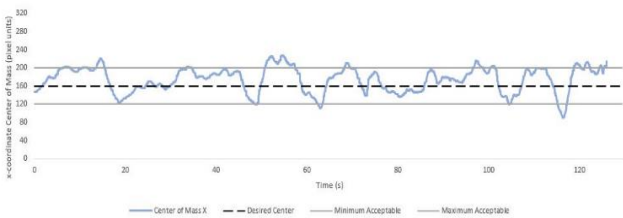


Figure 21. Center of Mass Data for Trial 2 Red.

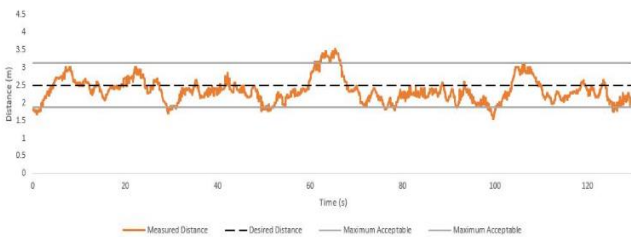


Figure 22. Measured Distance Data for Trial 2 Red.

Figures 19 and 21 show the positions of the center of mass of certain trials. The desired center of mass must be located at the center of the frame (broken line) and a range $\pm 25\%$ of the desired value (solid gray line) is set. Centers of mass positions within this range are considered to be acceptable.

Figures 20 and 22 show the measured distance of the hexacopter from the target for certain trials. The

desired distance must be maintained at 2.5 meters (broken line) and an acceptable range is set to be $\pm 25\%$ of desired distance (solid gray line).

The hexacopter was able to follow the selected target 80% of the time in this major test. The colors used were dark blue, green, light blue and red. The overall accuracy obtained is 64.25% and 79.85% for center and distance. This is relatively lower than the previous testing set-up's since the target is not fixed to a single color anymore. This would affect the overall performance of the system since it is possible that the algorithm will not be able to completely capture the target object because of the uneven lighting condition in the room. This lighting condition greatly affects the color seen from the camera. Furthermore, the lower accuracy may be caused by the activation of the obstacle avoidance algorithm. Since the priority is the obstacle avoidance algorithm, the accuracy of maintaining the distance and the center will drop during the target following. Among the trials, the most number of failed tracking happened when the selected target is color red (3 out of 5). A tracking failure may eventually happen since the lighting in some parts of the room cannot be controlled, and thus the detected target may be lost.

Figures 23 and 24 show the individual accuracies in maintaining the center of mass and the distance within the acceptable range of each trial for different shirt colors.

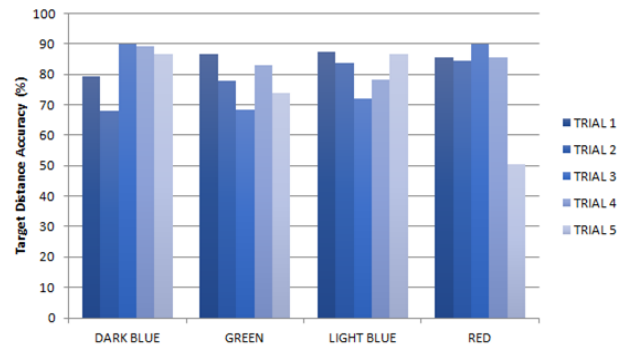


Figure 23. Target Center Accuracy for Major Test 3.

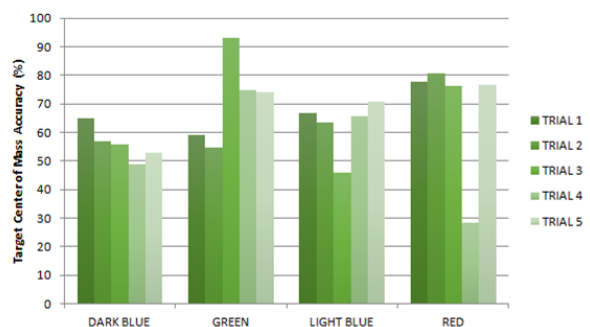


Figure 24. Target Distance Accuracy for Major Test 3.

The reliability of the system depends on the number of times the hexacopter was able to maintain tracking and following the object within two minutes, while the accuracy depends on the ability of the system to maintain the center of mass and the distance at a specified range. The developed algorithm was able to provide a reliability of about 90% with an overall accuracy of 76.23% for maintaining its distance from the object, and 74.46% for maintaining its position centered relative to target object location. The system has demonstrated satisfactory performance on small changes in illumination. Tables 3 and 4 shows the overall and individual accuracy and reliability of the system for each major test.

Table 3. Overall Accuracy.

Major Test	Center of Mass Accuracy (%)	Distance Accuracy (%)
1	81.11	63.43
2	75.01	85.42
3	64.25	79.85
Overall	73.46	76.23

Table 4. Overall Reliability.

Major Test	Total Number of Successful Trials	Total Number of Trials	Reliability (%)
1	15	15	100
2	6	6	100
3	16	20	80
Overall	37	41	90.24

Conclusions and Recommendations

An autonomous indoor navigation system of a hexacopter was developed, demonstrated and characterized in this research paper. The motion of the hexacopter is dictated by vision-based object tracking and an obstacle avoidance mechanism utilizing ultrasonic sensors. The system employs an NI myRIO embedded device for image processing and automation, and a Pixhawk flight controller for navigation. Together with the system, the developed LabVIEW Program connects with the hexacopter through the NI myRIO's built-in WiFi and allows the user to select a target object for tracking and observe the navigation of the hexacopter through the live video feed.

For this research of automating UAV navigation for indoor application, the NI myRIO has provided a lot of advantages and disadvantages. While the myRIO has provided the availability of LabVIEW which simplified many of the processes, the hardware itself became a limitation: the processor is not powerful enough to simultaneously perform image processing, tracking

calculations and path planning. It is therefore recommended that: (1) better and a more efficient algorithm be made, or (2) the employ of other embedded devices with better processors.

For future studies, the researchers suggest the recreation of the system with a different configuration: (1) using a faster processor and (2) employing different sensors that could provide better performance. In obstacle avoidance, adopting different sensor fusion techniques as well as to use different types of sensors designed for this application should be considered. As this research was able to implement color thresholding for detection and tracking, future work is to improve the object detection and tracking algorithms by making them more efficient and much more suitable for use on embedded devices. Another future work is to implement the works of this study to different types of UAVs such as fixed-plane, single-rotors, and hybrid models, expanding the capabilities of UAVs for many different applications.

Acknowledgment

This study was supported by the Philippine Government's Department of Science & Technology - Philippine Council for Industry, Energy and Emerging Research & Development (DOST-PCIEERD) with Project No. 04254, and the De La Salle University - University Research Coordination Office (DLSU-URCO) with Project No. 01 IR 1TAY16-1TAY17.

References

- [1] A.M. Garcia, M.A. Rufino, L.C. Sangalang, J.A. Teodoro, and J. Ila, "Application of Histogram of Oriented Gradient in Person Detection from Aerial Images," in De La Salle University Research Congress, Manila, Philippines, March 6-8, 2014.
- [2] D.M. Jr. Sobers, G. Chowdhary and E.N. Johnson, "Indoor navigation for unmanned aerial vehicles," In AIAA Guidance, Navigation, and Control Conference, Chicago, Illinois, 10-13 August 2009. <https://doi.org/10.2514/6.2009-5658>
- [3] Pixhawk overview. <http://pixhawk.org/> [Accessed 3 February 2018]
- [4] A.S. Putera and F. Ramdani, "Software Testing by Standard Software Metrics Method; Study Case 'Mission Planner' as UAV Ground Station Software," Journal of Telecommunication, Electronic and Computer Engineering, Vol 10, No. 1-8, pp. 123-128, 2018.
- [5] N.M. Kwok, Q. Ha & G. Fang, "Effect of Color Space on Color Image Segmentation," in 2nd International

Congress on Image and Signal Processing, IEEE Press, pp. 1-5, October 17-19, 2009.

<https://doi.org/10.1109/CISP.2009.5304250>

[6] A. Vadivel, M. Mohan, S. Sural, and A.K. Majumdar, "Segmentation Using Saturation Thresholding and Its Application in Content-Based Retrieval of Images, Image Analysis and Recognition," Lecture Notes in Computer Science, Vol. 3211, Berlin, Heidelberg: Springer, 2004.

https://doi.org/10.1007/978-3-540-30125-7_5

[7] H. Kadouf and Y. Mustafah, "Colour-based Object Detection and Tracking for Autonomous Quadrotor UAV". IOP Conference Series: Materials Science and Engineering, Vol. 53, 2013

<https://doi.org/10.1088/1757-899X/53/1/012086>

[8] P. Singh, B.B.V.L. Deepak, T. Sethi, M.D.P. Murthy, "Real-Time Object Detection and Tracking Using Color Feature and Motion," in International Conference on Communications and Signal Processing (ICCSP), Melmaruvathur, India, pp. 1236-1241, 2-4 April 2015

<https://doi.org/10.1109/ICCSP.2015.7322705>

[9] L. Wang, N. Liu, J. Wang, J. Hu, and F. Liang, "Design of an Intelligent Vehicle Control System Based on LabVIEW," Metallurgical & Mining Industry, Issue 7, pp. 21-27, 2015

[10] T. Shearwood. (2015), "Samaritan: an unmanned aerial vehicle for humanitarian aid missions,"

[Online]. Available:

<https://forums.ni.com/t5/LabVIEW-Student-Design/Samaritan-An-Unmanned-Aerial-Vehicle-for-Humanitarian-Aid/ta-p/3538053>

[Accessed: 5 February 2018]

[11] National Instruments. LabVIEW PID and Fuzzy Logic Toolkit User Manual. [Online]. Available:

<http://www.ni.com/pdf/manuals/372192d.pdf>

[Accessed: June 2009]

[12] A. Rosebrock (2015) "Find distance from camera to object/marker using Python and OpenCV,"

[Online] Available:

<https://www.pyimagesearch.com/2015/01/19/find-distance-camera-objectmarker-using-python-opencv/>

[Accessed: 19 January 2015]

[13] B. Taylor (2016) "Bolder Flight Systems SBUS,"

[Online]. Available:


<https://www.arduino-libraries.info/libraries/bolder-flight-systems-sbus>

[Accessed 3 December 2016]

[14] Radiolink, "Radiolink R12DS 12-CH 2.4GHz DSSS & FHSS Receiver," [online] Available:

<http://radiolink.com.cn/doce/product-detail-126.html> [Accessed: 3 February 2018]

Publisher: Chinese Institute of Automation Engineers (CIAE)
ISSN: 2223-9766 (Online)

 **Copyright:** The Author(s). This is an open access article distributed under the terms of the [Creative Commons Attribution License \(CC BY 4.0\)](https://creativecommons.org/licenses/by/4.0/), which permits unrestricted use, distribution, and reproduction in any medium, provided the original author and source are cited.